第 27 卷第 10 期 无 机 化 学 学 报 Vol.27 No.10
2011 年 10 月 CHINESE JOURNAL OF INORGANIC CHEMISTRY 2053-2060

微生物诱导碳酸钡沉淀

竹文坤[1,2] 罗学刚*[,2] 张 驰[2] 周 建[2]
([1]西南科技大学国防科技学院,绵阳 621010)
([2]生物质材料教育部工程研究中心,绵阳 621010)

摘要：利用巴斯德芽孢杆菌繁殖过程产生的酶化作用,适时引入 Ba^{2+},形成碳酸钡沉淀,通过用 X 射线粉末衍射(XRD)、扫描电子显微镜(SEM)、傅里叶变换红外光谱(FTIR)、综合热分析仪(DSC-TG)对碳酸钙样品形貌、结构、热性质等进行表征。结果表明,巴斯德芽孢杆菌诱导沉淀的碳酸钡与纯水中的不同,含有少量有机物质,晶形转变温度降低。主要为花簇状和放射状,属于正交晶系。菌体和代谢物在碳酸钡晶体成核、生长及堆积过程中扮演重要的角色。

关键词：巴斯德芽孢杆菌；碳酸钡；生物矿化
中图分类号：O614.23[+]3 **文献标识码**：A **文章编号**：1001-4861(2011)10-2053-08

Microbiological Precipitation of Barium Carbonate

ZHU Wen-Kun[1,2] LUO Xue-Gang*[,2] ZHANG Chi[2] ZHOU Jian[2]
([1]*School of National Defense Science and Technology, Southwest University of Science and Technology, Mianyang, Sichuan* 621010, *China*)
([2]*Engineering Research Center of Biomass Materials of China Ministry of Education,Southwest University of Science and Technology, Mianyang, Sichuan* 621010, *China*)

Abstract: The barium carbonate precipitate was induced using enzymes in the bacillus pasteurii reproduction and morphology, structure and thermal decomposition properties of the barium carbonate precipitates were characterized by SEM, FTIR, XRD, DSC-TG. The results indicate that barium carbonate ($BaCO_3$) precipitate induced in bacillus pasteurii differs from the one induced in pure water. The $BaCO_3$ crystals induced in bacillus pasteurii has orthorhombic crystalline structure and contains a small amount of organic matters, its crystal transition temperature decreases and shows morphologies of flower clusters and radial patterns. Bacteria and metabolites play important roles in the process of crystal nucleation, growth and accumulation of $BaCO_3$.

Key words: bacillus pasteurii; barium carbonate; biological mineralization

0 Introduction

Biological mineralization as a common phenomenon in nature is a process of solid phases of various materials with special advanced structures assembled in biological systems. During this process, organic macromolecules and inorganic ions interact in the inter-phase which enables the biogenic mineral to have the special multistage structure and assembly regulating inorganic mineral face separated from molecular horizontal[1-4]. Taking the biological macromolecules as a template, the biogenic minerals finally form

收稿日期:2011-03-03。收修改稿日期:2011-05-30。
国家“十一五”科技支撑计划课题(No.2007BAB18B08) 资助项目。
*通讯联系人。E-mail:lxg@swust.edu.cn

highly ordered inorganic-organic composite materials through the processes of molecular pre-assembly, interphase molecular recognition, growth modulation and cell processing. Because structure, shape consistent, crystal orientation and size for this kind of composite are special, biological minerals have various great functions[5-8]. Therefore, it is of great significance and attractiveness as promising prospect to simulate a biological mineralization of such kind of materials in organism.

Bacteria play an important role in the process of natural mineralization and deposition such as the deposition of carbonate in earth crust and the formation of rock[9-10]. They participate in and induce the formation of inorganic minerals, and they also have an extensive capacity of mineralization and deposition for phosphate, sulfate, carbonate, silicate, sulfide and oxides[11-12]. In recent years, bacterial induced mineralization has aroused the attraction of scholars in many fields [13-14], such as pollution control of heavy metal from groundwater, bioremediation of environmental pollution from heavy metal and property improvement of sand project.

As an important inorganic chemical raw material, barium carbonate is widely used in the field of ceramics, glass, magnetic material, microelectronic devices and superconductors[15-18]. In the structural ceramics production, powdered barium carbonate could reduce bubble stomata in the ceramics and improve the hardness of brick, wear resistance and chemical corrosion resistance. Because of its high dielectric constant and good temperature characteristics, mixing barium carbonate into the ceramic capacitor could make the capacitor be of small size, lightweight, large capacity and high frequency characteristics[19]. Mixing barium carbonate into the ferrite can improve their magnetic properties[20]. Especially in glass manufacturing, as baking additives, barium carbonate can increase the castability of glass and improve the quality of glass. As a result, the glass could have higher refractive index, greater hardness and can more effectively absorb X-ray shed produced by the high voltage, which is important to the production of color picture tube and computer monitors [21-22]. Hence, the preparation of barium carbonate powder has caused intensive research interests due to its important application prospects.

With the development of science and technology, the requirements towards the quality of the barium carbonate become higher and higher. Scientists pay intensive attention to the research of $BaCO_3$ crystal control. Different application fields require different shapes of barium carbonate crystals. There are many ways to prepare $BaCO_3$ crystals and to control the shape and morphology, such as liquid precipitation, micro emulsification, low temperature solid phase synthesis, template method, ultrasonic chemical method, microwave assisted synthesis and super gravity method [23-25]. As a new method, microbial deposition has couple of advantages such as resourcefulness, environment-friendliness and low cost. Long et al.[26] reported $BaCO_3$ synthesis by proteus mirabilis in Urea-$BaCl_2$ cultivation liquid. $BaCO_3$ particles change from oval to rod in morphology within 7 days of reaction, but their structure is still amorphous even after a month. The formation of barium carbonate is a slow process. In this paper, the appropriate carbonate mineralization bacteria has been selected, for example the use of the enzymatic effect in the growth and reproduction process to decompose urea, the addetion of Ba^{2+} to form $BaCO_3$ in a certain time, which has a nano-level crystal whisker on it′s surface. The mechanism has been studied.

1 Experimental

1.1 Materials

All of chemicals were analytical grade and used without further purification. Bacillus pasteurii (purchased from ATCC) was selected to investigate microbe induced calcite precipitation. Bacillus pasteurii was inoculated on beef extract peptone culture (10 g beef extract, 5 g peptone, 5 g sodium chloride and 15 g agar were dissolved in Milli-Q water to 1 L and pH value was adjusted to 8.0), cultivated at 30 ℃ for 24 h and then kept in refrigerator at 4 ℃ for stock. Bacillus pasteurii was also inoculated into liquid seed medium

(20 g glucose, 10 g peptone and 10 g sodium chloride were dissolved in Milli-Q water to 1 L and the pH value was adjusted to 8.0), incubated at 30 ℃ for 24 h in a shaker running at 160 r·min^{-1} and then kept in refrigerator at 4 ℃ for stock.

The instruments used were listed as follows: S440 scanning electron microscope (SEM, Leica Cambridge LTD, UK), Nicolet-6700 Fourier infrared spectroscope (FTIR, American Nicolet Corporation, USA), X'Pert PRO X-ray diffraction (XRD, PANalytical B.V., USA), Q500 Thermogravimetry analyzer (TGA, American TA Corporation, USA).

1.2 Methods

100 mL of 1 mol·L^{-1} $Ba(NO_3)_2$ and 20 g·L^{-1} urea solutions were prepared. The above solutions were mixed and stirred. A small amount of urase was added into the solution, stirred for 10 min, stood for 48 h at 30 ℃. The product was filtrated and washed three times with Milli-Q water and ethanol, and then dried at 45 ℃ for 24 h. The powder samples were collected.

1 L of liquid medium was prepared using Milli-Q water, glucose 20 g, peptone 10 g, NaCl 5 g and shook to a clear solution which then was adjusted pH value to 8.0 using 0.1 mol·L^{-1} HCl or NaOH aqueous solution. 250 mL ready medium was added in a 500 mL flask bottle and sterilized. The liquid media was made in triplicate using the above procedure and kept in three bottles, marked by #1 to 3. 10 mL of 20 g·L^{-1} urea aqueous solution was dropped into each bottle containing the ready medium after filtration and sterilization. Further, 10 mL liquid strains was added to each bottle and cultivated in the oscillation incubator (160 r·min^{-1}) at the temperature of 30 ℃ for 48 h. The active bacteria density was 5.94×10^9 cfu·mL^{-1}, then 100 mL of 1 mol·L^{-1} barium nitrate solution was introduced. After stirring for 10 min, each bottle was stood for 10 min, 1 d and 4 d, respectively. The products were filtrated and washed three times with Milli-Q water and ethanol, and then dried at 45 ℃ for 24 h. The powder samples were collected.

1.3 Analysis of sample

The morphology of the products was observed by the scanning electron microscope (SEM) with magnifying from 1000 to 10000. The crystal structure of the product was analyzed by X-ray diffraction (XRD), which used a tube voltage of 40 kV and current of 100 mA with Cu $K\alpha$ radiation of 0.154 056 nm. The scanning angle range from 3° to 80° with the step at 0.02°. The IR spectrum of the product was recorded by KBr pellet technique with the resolution of 4 cm^{-1}. Scanning the product for 20 times with the range of 4 000~400 cm^{-1}. The thermal properties of the products were investigated by DSC-TG composite thermo-analytical instrument in the elevated tempera-ture range of 50 ℃ to 1 450 ℃ at a ramp of 20 ℃·min^{-1}.

2 Results and discussion

2.1 XRD and FTIR analysis

The FTIR spectra of obtained $BaCO_3$ precipitate induced in pure water system and in bacillus pasteurii are shown in Fig.1. Fig.1(a) shows characteristic absorption peaks of $BaCO_3$ precipitate induced in pure water mainly at 3 434 cm^{-1}, 1 455 cm^{-1}, 857 cm^{-1} and 693 cm^{-1}. The broad absorption peak of 3 434 cm^{-1} is assigned to -OH bond symmetric stretching vibration and asymmetric stretching vibration due to the existence of hydroxyl and adsorbed water on the surface of $BaCO_3$ particles. The peaks at 857 cm^{-1} and 693 cm^{-1} are in-plane bending vibration and the out-plane bending vibration of CO_3^{-2}, and the peak at 1 455 cm^{-1} is asymmetric stretching vibration of C-O[26-28], which are all typical peaks of $BaCO_3$ particles. The IR spectra of $BaCO_3$ precipitate induced in bacillus pasteurii

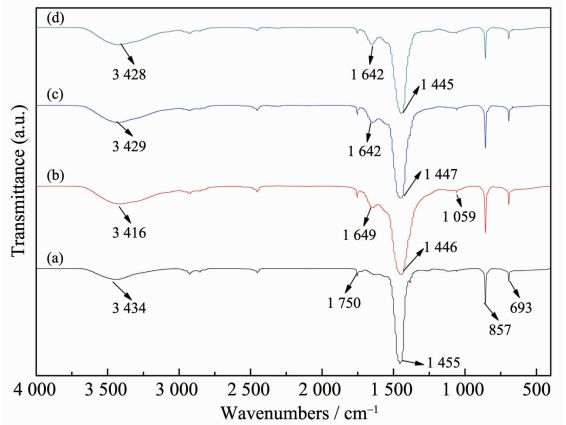

Fig.1 FTIR spectra of the $BaCO_3$ particles induced in (a) pure water; induced in bacillus pasteurii for (b) 10 min, (c) 1 d and (d) 4 d, respectively

at different times are shown in Fig.1 (b~d), which were almost similar. Compared with the absorption peak of the $BaCO_3$ precipitate induced in pure water system at 3 434 cm^{-1} and 1 455 cm^{-1}, two peaks shift towards lower band, which is perhaps due to the strong interaction between biomass, metabolites and $BaCO_3$ salt. There are new absorption peaks at 1 642 cm^{-1} and 1 059 cm^{-1} assigned to amide Ⅰ band (primary from C=O stretch) and C-O stretching vibration [29-32], showing preliminarily barium carbonate sample containing a small amount of organic species from bacteria and metabolites.

The XRD patterns of $BaCO_3$ precipitate induced in pure water system and induced in bacillus pasteurii are shown in Fig.2. Fig.2 (a~d) show that though the sizes or crystal forms of the four particles are different, their diffraction peak position and intensity are similar. Compared the data of PDF standard cards (No.5-0586), locations of the main diffraction angles for each sample (2θ=19.4°, 23.9°, 27.4°, 34.0°, 42.2°, 44.6°, 46.8°, 55.6°, 60.9°, 67.8°, 76.8°) correspond to crystal faces of (101), (111), (002), (022), (032), (310), (311), (331), (401), (224) and (510) plane, respectively(Fig.2(d)). The peak position and peak intensity are in good agreement with diffraction data of PDF (No.5-0506) quadrature phase $BaCO_3$ (a=0.625 nm, b=0.883 nm, c=0.654 nm). It turns out that the samples are all quadrature phase of the $BaCO_3$. The characteristics of the samples from the sharp diffraction peaks and very narrow half-peak width imply that the crystallization was basically complete but the crystals grow into larger size.

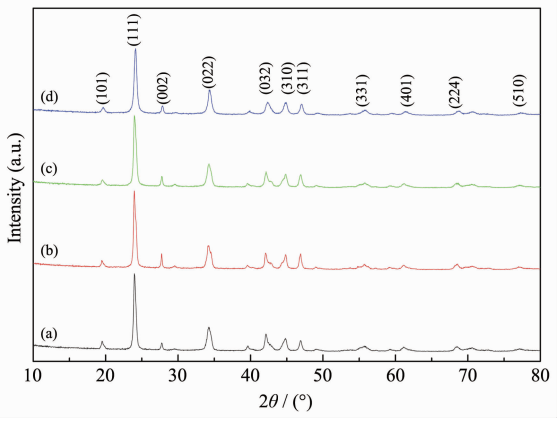

Fig.2 XRD patterns of the $BaCO_3$ particles induced in (a) pure water; $BaCO_3$ particles induced in bacillus pasteurii for (b) 10 min, (c) 1 d and (d) 4 d, respectively

2.2 SEM analysis

The morphology of barium carbonate produced by pure water system and by bacillus pasteurii inducement is shown in Fig.3. Fig.3a shows that linear $BaCO_3$ precipitate induced in pure water system with aspect ratio between 4∶1 and 8∶1, and the particles are hexagonal-shaped in cross section, size range between 100 and 300 nm in diameter and well dispersed without agglomeration.

The growth of $BaCO_3$ crystals exhibits certain continuity (Fig.3(b~d)). After 10 min of induced precipitation in bacillus pasteurii aqueous, the morphology of $BaCO_3$ particles showed the flower cluster, radial and small cylindrical patterns, with good dispersion at particle size between 1~5 μm (Fig.3(b)). After induced precipitation in bacillus pasteurii for 1 day, part of the $BaCO_3$ particles is agglomerated, columnar $BaCO_3$ particles disappeared, instead, the main morphologies are the flower cluster and radial patterns at particle size between 5~10 μm (Fig.3(c)). For longer time induction in bacillus pasteurii aqueous, the flower cluster and radial patterns of $BaCO_3$ particles combine into some whole clog/aggregates at the diameter range between 10 and 20 μm for 4 days, and there are many crystal whiskers on the surface of clog/aggregates. These crystal whiskers link with each other and exhibit columnar pattern at diameter range between 50 and 200 nm (Fig.3(d~e)).

2.3 TG/DSC analysis

Fig.4 shows the TG/DSC curves of $BaCO_3$ particles. Fig.4(a) is the TG/DSC curve of barium carbonate particle induced in pure water. TG curves show that the weight loss step appears at the temperature between 50 ℃ to 800 ℃, and the weightlessness rate was about 1.395%, which could be attributed to the evaporation of adsorption water in the sample. When the temperature increases over 800 ℃ but less than 1 000 ℃, two endothermic peaks appear at 814.03 ℃ and 977.75 ℃ in the DSC curves, respe-ctively. It is believed that there is certain phase transition or chemical reaction occurring in this process. According to the character of

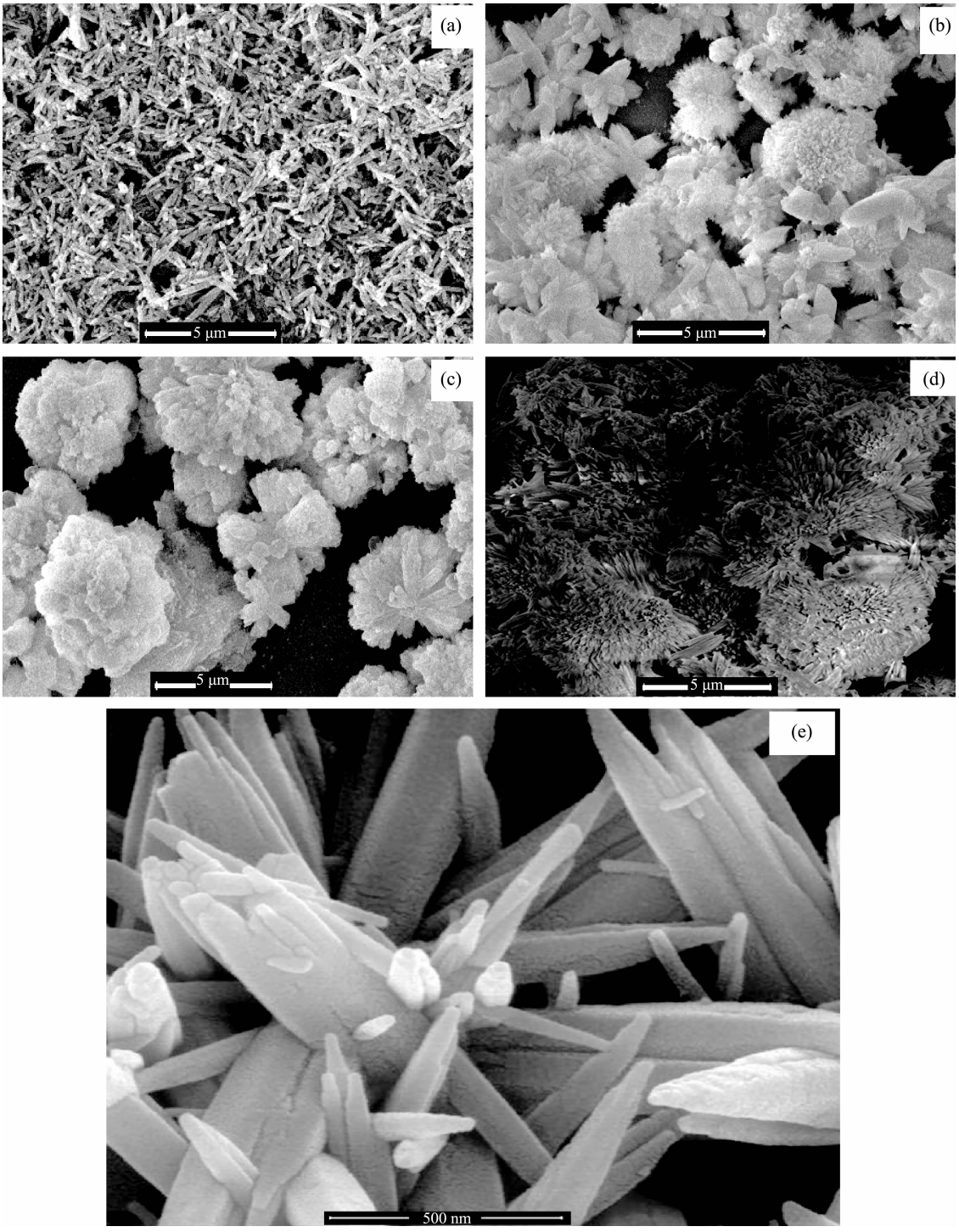

Fig.3　SEM images of the $BaCO_3$ particles induced in (a) pure water; $BaCO_3$ particles induced in bacillus pasteurii for (b) 10 min, (c) 1 d and (d) 4 d, respectively

pure barium carbonate, 818.52 ℃ is the phase transition temper-ature point with a transit from γ-phase to β-phase, and 978.89 ℃ is another phase transition temperature point from β-phase to α-phase which fits on the basic line of theoretical value (from normal temperature to 811 ℃ is at γ-phase, 811~982 ℃ at β-phase and above 982 ℃ at α-phase) [22-33]. We therefore convince that the two endo-thermic peaks at 814.03 ℃ and 977.75 ℃ are the corresponding phase transition temperatures, namely, (γ-phase to β-phase) and (β-phase to α-phase), respectively. TG curves decline sharply at the temperature range between

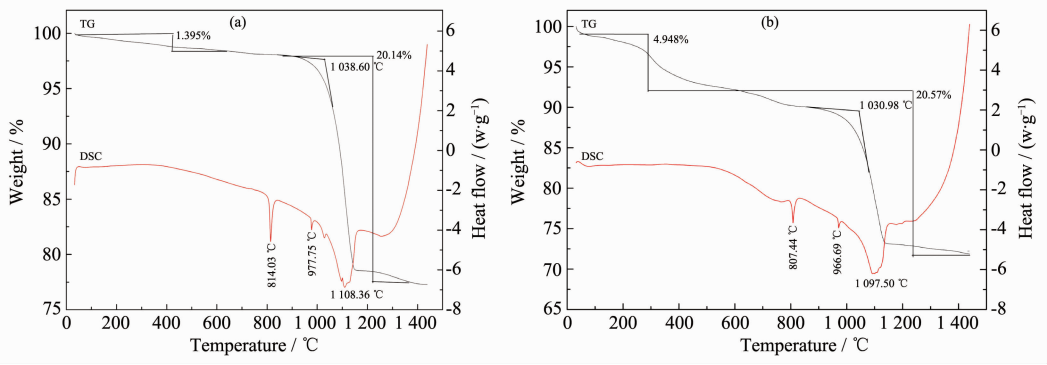

Fig.4 TG/DSC curves of the $BaCO_3$ particles induced in (a) pure water, (b) bacillus pasteurii for 4 d

1 000~1 400 ℃ at a weightlessness rate about 20.14% with a remarkable endothermic peak in this temperature range due to the outcome of its decomposition[22,33].

Fig.4(b) is the TG/DSC curve of $BaCO_3$ particles induced in bacillus pasteurii for 4 d. There is a weight loss step in the temperature range between 50~600 ℃, and the weightlessness rate is 4.948% . It may be caused by evaporation of adsorbed water in the sample and decomposition of organic species such as proteins introduced in growth of $BaCO_3$ crystals induced in bacteria. When temperature is increased over 800 ℃ but less than 1 000 ℃, two endothermic peaks appear at 807.44 ℃ and 966.69 ℃ , respectively. The former belongs to (γ-phase to β-phase) transition temperature and the latter belongs to (β-phase to α-phase) transition temperature[22,33]. DSC curves also decrease in the temperature range between 1 000~1 400 ℃ where there is a noticeable endothermic peak corresponding to a TG weightlessness rate about 20.57% , the endo-thermic band is attributed to the decomposition of barium carbonate [22,33]. The experiment shows that under a high-temperature calcinating condition, the phase transition temperatures of $BaCO_3$ particles induced in bacillus pasteurii are shifted to lower range but the weightlessness rate is less than that of its counterpart, indicating the composition and structure of the $BaCO_3$ crystals induced in bacteria are significantly different from its counterpart induced in water.

2.4 Discussion of mechanism

Biological mineralization is widespread in nature. Biological mineralization differs obviously from geological mineralization because the crystallization of inorganic phase is strictly controlled by the organic species secreted by organism.The most organic species are water insoluble organic matter (IM) which usually consists of a number of water-repellent molecules such as chitin and silk protein. The rest organic species contain small amount of water soluble organic matter (SM) which normally consists of acidic proteins, glycoprotein, protein, etc. The polysaccharide parts of the SM are sulfate-rich. SM is a major controller and regulator of biological mineralization[6,34].

Bacillus pasteurii is vaccinated into medium and utilizes urea as nutrient. The urea is constantly decomposed by emzymolysis, causing the increase of solution pH value and more suitable environment to the growth. Reproduction of bacteria and the emzymolysis were enhanced continuously. In this circular process, the CO_3^{2-} concentration in solution is increased with the continuous depositions of urea. Negatively charged water-soluble organics on the surface of microbial cells chelate Ba^{2+} constantly, inducing higher concentration of CO_3^{2-} locally and more Ba^{2+} are reacted with CO_3^{2-} until crystal precursor concentration increases enough for nucleation and precipitation of $BaCO_3$ particles. Small grains are formed in the early precipitation then the small grains pile up together with each other to form larger particles for a longer period of time due to the microbial cells chelate Ba^{2+} until forming radial aggregates. The possible biochemical reactions to induce $BaCO_3$ precipitation on bacterial cell surface in urea-$Ba(NO_3)_2$ medium could be summarized as follows[34-35].

$$NH_2\text{-}CO\text{-}NH_2+3H_2O \rightarrow 2NH_4^++2OH^-+CO_2$$

$$Ba^{2+}+Cell \rightarrow Cell\text{-}Ba^{2+}$$

$Cl^-+HCO_3^-+NH_3=NH_4Cl+CO_3^{2-}$

$Cell\text{-}Ba^{2+}+CO_3^{2-} \rightarrow Cell\text{-}BaCO_3\downarrow$

Microbiologically-induced $BaCO_3$ precipitation is recognized as a more complicated process than chemically-induced one. The surface of microbial cells contains plenty of ions which serve as nucleation sites to nonspecifically induce the precipitation of minerals[36]. Especially, Ba^{2+} is unlikely utilized by microbial metabolism but accumulated extracellularly[37]. Therefore, the negatively charged monolayer is the most favorable to crystal nucleation and growth.

3 Conclusions

(1) The morphology of $BaCO_3$ precipitates induced in bacillus pasteurii differs from that induced in pure water. The crystals induced in the bacteria aqueous have orthorhombic crystalline structure caused by a small amount of organic species. Due to the presence of the organics, $BaCO_3$ morphology shows flower clusters and radial patterns and the crystal transition temperature of $BaCO_3$ decreases.

(2) Due to the microbial cells chelate Ba^{2+} and longer time period for $BaCO_3$ precipitation, the growth of $BaCO_3$ crystals has a character of continuity. Small grains are piled up together with each other to form larger particles for a longer period of time due to the microbial cells chelate Ba^{2+} until forming radial aggregates.

Acknowledgement: This work was supported by Key Projects in the National Science & Technology Pillar Program during the Eleventh Five-year Plan Period (No.2007BAB18B08) and Postgraduate Innovation Fund sponsored by Southwest University of Science and Technology (No.10ycjj23).

References:

[1] CAI Guo-Bin(蔡国斌), YU Shu-Hong(俞书宏). *Chin. Bull. Life Sci.*(*Shengming Kexue*), **2008**,**20**(3):331-336

[2] Arias J L, Fernández M S. *Mater. Charact.*, **2003**,**50**:189-195

[3] Yu J, Yu J, Guo Z X. et al. *Macromol. Rapid Commun.*,**2001**, **22**:1261-1264

[4] Donners J J M, Brigid R H, Meijer E W. et al. *Chem. Commun.*, **2000**,**19**:1937-1938

[5] Kensuke N, Yoshiki C. *Chem. Mater.*, **2001**,**13**:3245-3259

[6] Berman A, Addadi L, Weiner S. *Nature*, **1988**,**311**(11):546-548

[7] LU Peng(鲁鹏), HOU Shan-Hua(侯善华), OUYANG Jian-Ming(欧阳健明). *Chinese J. Inorg Chem.* (*Wuji Huaxue Xuebao*), **2010**,**1**(26):17-24

[8] WANG Run-Xia(王润霞) , XIE An-Jian(谢安建), LI Shi-Kuo (李士阔). *Chinese J. Inorg Chem.* (*Wuji Huaxue Xuebao*), **2009**,**25**(10):1711-1716

[9] Ben-Chekroun K B, Rodríguez-Navarro C, González-Munoz M T, et al. *J. Sediment. Res.*, **2004**,**74**:868-876

[10]Rodriguez-Navarro C, Jimenez-Lopez C, Rodriguez-Navarro A, et al. *Geochim. Cosmochim. Acta*, **2007**,**71**:1197-1213

[11]Van Lith Y, Warthmann R, Vasconcelos C, et al. *Sedimentology*, **2003**,**50**:237-249

[12]Rivadeneyra M A, Martin-Algarra A, Sanchez-Navas A, et al. *Geomicrobiol. J.*, **2006**,**23**:89-101

[13]Mitchell A C, Ferris F G. *Geochim. Cosmochim. Acta*, **2005**, **69**:4199-4210

[14]Jason T D, Michael B F, Klaus N J. *Geotech. Geoenv.*, **2006**, **132**:1381-1392

[15]Chem P C, Cheng G Y, Kou M H, et al. *J. Cryst. Growth.*, **2001**,**226**:458-472

[16]Yu S H, Cölfen H, Xu A W, et al. *Cryst. Growth Des.*, **2004**,**4**: 33-37

[17]Guo X H, Yu S H. *J. Cryst. Growth*, **2007**,**7**:354-359

[18]Zheng N W, Wu Q H, et al. *Chem. Lett.*, **2000**,**6**:638-639

[19]Kuang D B, Xu A W, et al. *J. Cryst. Growth*, **2002**,**244**:379-383

[20]Sondi I, Matijevic E. *Chem. Mater.*, **2003**,**15**:1322-1326

[21]Ni Y D, Zhang H Y, Hong J M, et al. *J. Cryst. Growth*, **2008**, **3**:4460-4467

[22]WANG Lin-Na(王丽娜), XIE Chang-Dong(谢长东), HUO Ji-Chuang(霍冀川). et al. *J. Synth. Cryst.* (*Rengong Jingti Xuebao*), **2010**,**39**:788-792

[23]LIU Shu-Xin(刘树信), HUO Ji-Chuan(霍冀川), YANG Ding-Ming(杨定明), et al. *J. Synth. Cryst.*(*Rengong Jingti Xuebao*), **2005**,**34**:531-535

[24]LIU Quan-Yong(刘全勇), JIANG Lei(江雷). *Chem. J. Chinese Universities* (*Gaodeng Xuexiao Huaxue Xuebao*), **2010**,**31**: 1065-1071

[25]GAO Hao-Yun(高远浩), NIU He-Lin(牛和林), et al. *Chinese J. Inorg Chem.*(*Wuji Huaxue Xuebao*), **2003**,**19**:37-40

[26]Long C, Yu H S, An J X. *Cryst. Growth Des.*, **2009**,**9**(2):743-754

[27]Pasierb P, Komornicki S, Rokita M, Rekas M. *J. Mol. Struct.*, **2001**,**596**:151-152

[28]Miller F A, Carlson G L, Bentley F F. *Spectrochim. Acta*, **1960**,**16**:135-136

[29]Arrondo J L R, Muga A, Castresana J, et al. *Prog. Biophys. Mol. Biol.*, **1993**,**59**:23-56

[30]Surewicz W K, Mantsch H H, Chapman D. *Biochemistry*, **1993**,**32**:389-394

[31]Pezolet M, Bonenfant S, Dousseau F, et al. *Febs. Lett.*, **1992**, **299**:247-250

[32]CHENG Liang(成亮), QIAN Chun-Xiang(钱春香), WANG Run-Xing(王瑞兴), et al. *Acta Chim. Sinica* (*Huaxue Xuebao*), **2007**,**65**(19):2134-2138

[33]Judd M D, Pope M I. *J. Therm. Anal.*, **1972**,**4**:31-38

[34]WANG Run-xing(王瑞兴), QIAN Chun-xiang(钱春香), WANG Jian-yun(王剑云). *J. Southeast Univ.* (*Dongnan Daxue Xuebao*), **2005**,**7**:191-195

[35]Tiano P. *Stud. Conserv.*, **1995**,**40**:171-176

[36]Ramachandran S K, Ramakrishnan V, Bang S S. *ACI. Mater. J.*, **2001**,**98**:3-9

[37]Lochhead M J, Letellier S R, Vogel V. *J. Phys. Chem.*, **1997**, **101**:10821-10827